Stellar Capture Rates in Galactic Nuclei Containing a Supermassive Binary Black Hole

Shashank Dattathri

UG Department
Indian Institute of Science

June 2020

Supervisor: Prof. Arun Mangalam
Indian Institute of Astrophysics

Introduction

- Supermassive black holes exist at the nucleus of nearly all galaxies.
- The study of the properties of SMBHs, their effects on the surrounding star cluster, and most importantly, their detection has been an active and rapidly evolving topic of research.
- Stars that wander too closely to the black hole can be captured by it. This can happen if the star enters the event horizon, or if it is tidally disrupted by the BH.
- Tidal disruption events (TDEs) can manifest themselves as a luminosity flare at the center of a galaxy for a few years, and the gas released from the disrupted star can be a source of power for quasars and AGN.
- Analytical works, numerical simulations, and observations have shown that the average TDE rate in most galaxies is $\sim 10^{-5} - 10^{-4}\ yr^{-1}$.

- According to the standard Λ cold dark matter paradigm of structure formation in the universe, galaxies grow through the merger of smaller galaxies.
- We focus on the mergers of unequal mass galaxies. If both the merging galaxies contain an SMBH, then after an initial stripping away of stars, the two black holes will form a bound system.
- In this work, we study the stellar capture rates in galactic nuclei containing an unequal mass binary black hole. Theoretical and numerical studies have shown that under the right conditions, there can be a two to three order of magnitude enhancement in the tidal disruption rate.
- Our study consists of a hierarchical system of a primary black hole, a secondary black hole, and a star in a stellar cusp surrounding the primary.

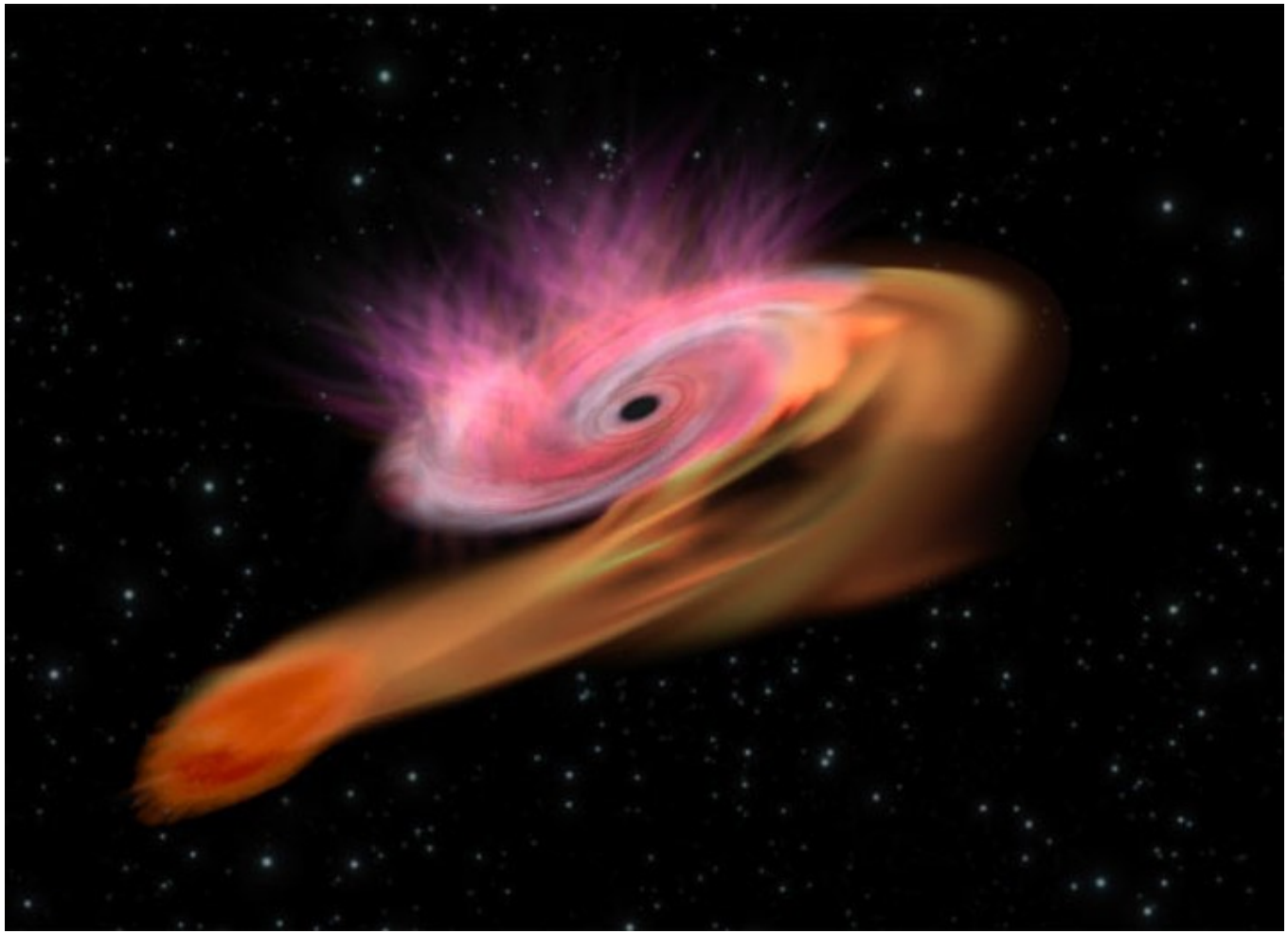

Figure: An artistic impression of tidal disruption of a star by a supermassive black hole. Image credit: ESA/C. Carreau.

Orbital Mechanics around Supermassive Black Holes

A two body system can be characterized using the Delaunay variables:

$$
\begin{aligned}
l &= M \\
h &= \Omega \\
g &= \omega \\
L &= \sqrt{ma} \\
H &= \sqrt{ma(1-e^2)}\cos i \\
G &= \sqrt{ma(1-e^2)}\ .
\end{aligned}
$$

These are derived from the action-angle variables for a spherical potential.

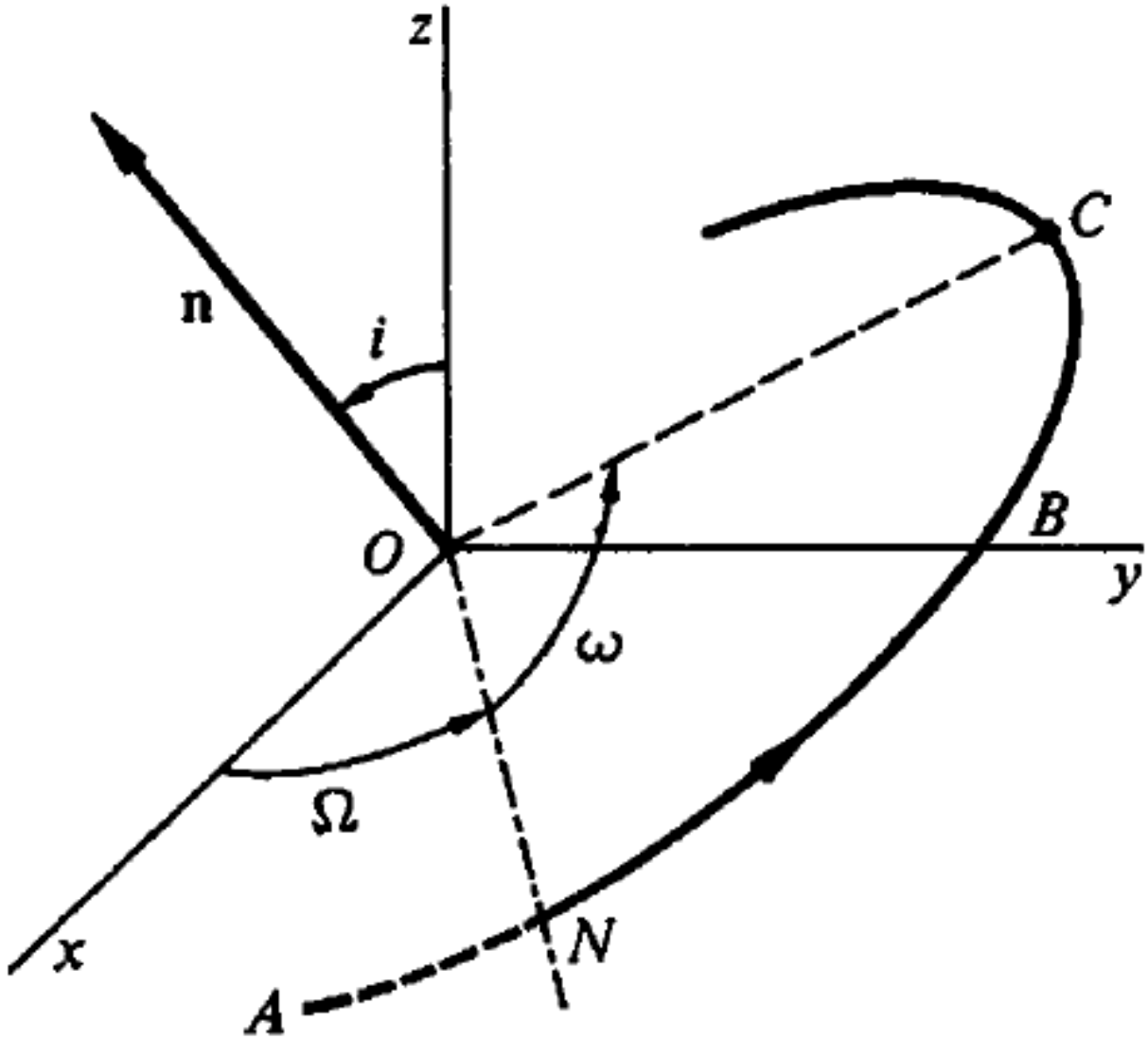

Figure: The Delaunay variables. C is the point of periapsis, and ON is the line of nodes. Figure taken from Goldstein et. al.

Lidov-Kozai mechanism

- The hierarchical three-body problem is a special case of the general three body problem in which the system consists of an inner binary which is perturbed by a distant object.
- Consider three bodies of mass M_1, M_2, and m. The mass ratio is $q = M_2/M_1$. Let r_1 and r_2 be the position vectors from M_1 to m and M_2, respectively, with $|r_1| < |r_2|$.
- In our system, we take the limit of $m << M_1, M_2$, i.e. the test particle limit. In effect, this reduces the system to an inner binary consisting of M_1 and m, and an outer binary consisting of M_2 orbiting the center of mass of M_1 and m. The body M_2 perturbs the orbit of m.
- The Hamiltonian of the mass m to quadrupolar approximation is:

$$H = -\frac{GM_1 m}{2a_1} - \frac{G(M_1 + m)M_2}{2a_2} - \frac{GM_1 M_2 m}{2(M_1 + m)} \frac{r^2}{r'^3}(3\cos^2\psi - 1)$$

where the subscript 1 refers to the inner binary, the subscript 2 refers to the outer binary, and ψ is the angle between the position vectors of the centers of the inner and outer binaries.

- We then employ the technique of secular averaging:

$$\overline{X} = \frac{1}{2\pi}\int_0^{2\pi} dE(1 - e\cos E)X[a(1 - e\cos E)]$$

  We average twice: once with respect to the inner orbit and then to the outer orbit.

- The resulting dimensionless Hamiltonian of the test particle m is:

$$H = \frac{1}{8}\left[-5 + 3I^2 + 3\sin^2 i(I^2 + 5e^2\sin^2\omega)\right]$$

  where $I = L/L_c$ is the dimensionless angular momentum and $\cos i = I_z/I$.

- We immediately see that since the Hamiltonian is cyclic in Ω, the conjugate momentum I_z is conserved.

- The equations of motion are:

$$\frac{d\omega}{d\tau} = \frac{\partial H}{\partial l} = \frac{3}{4l}\left[2l^2 + 5\sin^2\omega(e^2 - \sin^2 i)\right] ,$$
$$\frac{dl}{d\tau} = -\frac{\partial H}{\partial \omega} = -\frac{15}{8}e^2 \sin^2 i \sin(2\omega) ,$$
$$\frac{d\Omega}{d\tau} = -\frac{\partial H}{\partial l_z} = \frac{3}{4}\frac{\cos i}{l}(l^2 + 5e^2 \sin^2\omega) ,$$
$$\frac{dl_z}{d\tau} = \frac{da}{d\tau} = 0 ,$$

  where τ is in units of $T_K = \nu_0^{-1} = \frac{\sqrt{M_1}}{\sqrt{G}M_2}\frac{D^3}{a^{3/2}}(1 - e_2^2)^{3/2}$, the timescale of the oscillations. Here a is the semimajor axis of the field star m, and D is the separation between the black holes M_1 and M_2.

- In addition to l_z, there is a second conserved quantity due to the conservation of energy:

$$Q = e^2(5\sin^2 i \sin^2\omega - 2) .$$

There are two classes of orbits:

- Circulation in ω: These orbits have $\frac{d\omega}{d\tau} = 0$ at $\omega = 0, \pi$. They exhibit minimal variations in inclination and eccentricity.
- Libration in ω: These orbits have $\frac{d\omega}{d\tau} = 0$ at $\omega = \pm\frac{\pi}{2}$. They exhibit large oscillations in inclination and eccentricity, and are of more interest to us. The angular momentum can oscillate between $I \sim I_z$ to $I \sim 1$.
  Librating orbits require the existence of a fixed point at $\omega = \pm\frac{\pi}{2}$.
  The timescale of these oscillations is of the order of T_K.

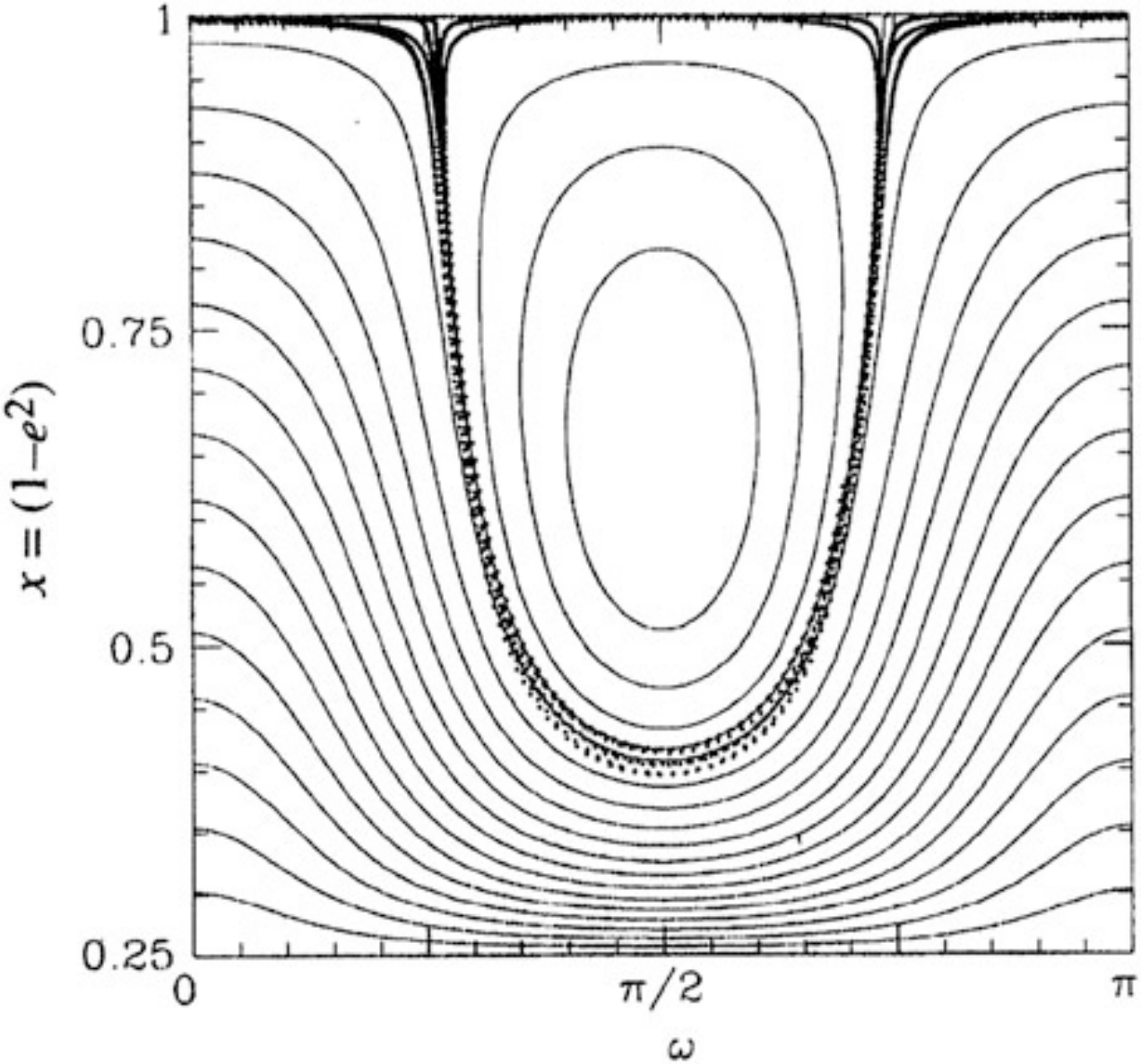

Figure: Circulating and librating orbits in the Lidov-Kozai mechanism. Figure taken from Shevchenko (2017).

Stellar Potential Precession

- The Lidov-Kozai mechanism faces competition from other sources of precession. We examine two major sources: stellar potential precession and general relativity precession.
- A stellar cluster around a SMBH perturbs the orbit of a star from the regular Keplerian ellipse.
- We assume a spherical cluster, where the density of the nucleus is represented by

$$\rho = \rho_0 \left(\frac{r}{r_0} \right)^{-\gamma} .$$

- The rate of precession due to this cusp is

$$\frac{d\omega}{dt} = -\nu G_M(e, \gamma) \sqrt{1 - e^2} \left[\frac{M_*(a)}{M_1} \right]$$

where $\nu = \frac{\sqrt{GM_1}}{a^{3/2}}$ is the unperturbed Kepler frequency, $M_*(a)$ is the mass of stars within a sphere of radius a, and $G_M(e, \gamma)$ is a numerical factor of order unity.

General Relativity

- General relativity effects of a Schwarzschild black hole induce precession of the pericenter of a stellar orbit.
- The precession rate is given by

$$\frac{d\omega}{dt} = \frac{3(GM)^{3/2}}{a^{5/2}(1-e^2)c^2} \ .$$

Loss Cone Dynamics

- The tidal radius for a star of mass m_* and radius r_* orbiting a black hole of mass M is

$$r_t = \left(\eta^2 \frac{M}{m_*}\right)^{1/3} r_* \ .$$

  where η is a factor of order unity.

- If $r_t > r_g$, the event horizon radius of the BH, then an observable tidal disruption event (TDE) is produced. On the other hand, if $r_t < r_g$, the star is swallowed whole into the BH without a TDE flare. For solar mass stars, this happens if $M \gtrsim 10^8 M_*$. We define captures to include both cases in order to derive a general formula for capture rate into the BH.

- An orbit with a periapsis of r_t has angular momentum equal to $L_{lc} = \sqrt{2r_t^2(E - \Phi(r_t))} \approx \sqrt{2GMr_t}$ (we assume that the orbit is highly eccentric). Orbits with $L \leq L_{lc}$ are called loss cone orbits, and the set of all loss cone orbits is called the loss cone.

- The diffusive or empty loss cone is when a star may wander in and out of the loss cone many times before capture. On the other hand, the pinhole or full loss cone is when a star is captured in a single orbital period.

Supermassive Binary Black Hole Evolution

The evolution of a binary black hole system can be categorized into three stages:

- Stage 1: Inspiral due to dynamical friction
- Stage 2: Formation of hard binary by ejection of stars
- Stage 3: Continued hardening by secondary slingshot and collisional loss cone repopulation

Stage 1: Dynamical friction stage

- The Chandrasekhar dynamical friction formula for the change in velocity of an object of mass M as it falls through a field of stars of mass m and velocity distribution function $f(v)$ is

$$\frac{d\mathbf{v}_M}{dt} = -16\pi^2 \ln\Lambda G^2 m(M+m)\frac{1}{v_M^3}\int_0^{v_M} v^2 f(v) dv \mathbf{v}_M \,,$$

  where $\mathbf{v}_M$ is the velocity of the object under consideration and $\ln\Lambda$ is the Coulomb logarithm.
- We consider that the secondary BH M_2 is inspirling into the primary BH M_1, while maintaining a nearly circular orbit. This is a reasonable assumption because dynamical friction tends to circularize orbits. As before, we assume a stellar density distribution which varies as $\rho = \rho_0(r/r_0)^{-\gamma}$.
- The binary separation as a function of time is then given by:

$$\frac{dr}{dt} = -\sqrt{\frac{GM_1}{r_0}}\frac{M_2}{M_1}\ln\Lambda\left(\frac{r}{r_0}\right)^{\gamma/2-2} F(\gamma) \,,$$

  where $F(\gamma)$ is a numerical factor of order unity.

Stage 2: Hardening stage

- When stars interact with a massive binary, they tend to gain energy and are scattered onto new orbits, or even escape the system completely. This mechanism is called the gravitational slingshot. The transfer of energy from the binary to the field stars is the driving force behind stage 2 in MBHB evolution.
- We define the binary hardening rate:

$$\mathcal{H} = \frac{\sigma}{G\rho}\frac{d}{dt}\left(\frac{1}{a}\right) .$$

  Simulations show that H can be expressed as $\mathcal{H} \approx q\mathcal{H}_\infty$ when $a \leq r_h$, where $\mathcal{H}_\infty \approx 16$.
- Phase 2 of the SMBHB ends when the binary separation reaches $\Delta r = a_h$, the hardening radius:

$$a_h = \frac{\mu}{M_{12}}\frac{r_h}{4} = \frac{q}{(1+q)^2}\frac{r_h}{4} .$$

Stage 3: Collisional Loss Cone Repopulation

- At $\Delta r \leq a_h$, the SMBHB evolution is facilitated by the loss cone repopulation of field stars.
- However unlike the earlier case of capture, a star which enters into the loss cone is not necessarily "lost"; they interact with the binary strongly enough to contribute to its evolution.
- The energy gained by the stars by this loss cone repopulation is compensated by the decrease in the binary's energy:

$$\frac{d}{dt}\left(\frac{GM_1M_2}{2a}\right) = -m_* \int \frac{N(\mathcal{E},t)}{P(\mathcal{E})}\langle\Delta\mathcal{E}\rangle d\mathcal{E} \qquad (1)$$

where $\langle\Delta\mathcal{E}\rangle$ is the average change in energy of the field stars per interaction.

- Integration of the above equation gives

$$\frac{a_h}{a(t)} = \sqrt{1+\mathcal{D}t} \qquad (2)$$

where $\mathcal{D} = \frac{G^2 m_* \mu}{4\sigma^2}\int_0^{\mathcal{E}_{crit}} \frac{N(\mathcal{E})\langle\Delta\mathcal{E}\rangle}{P(\mathcal{E})L_c^2(\mathcal{E})} d\mathcal{E}$.

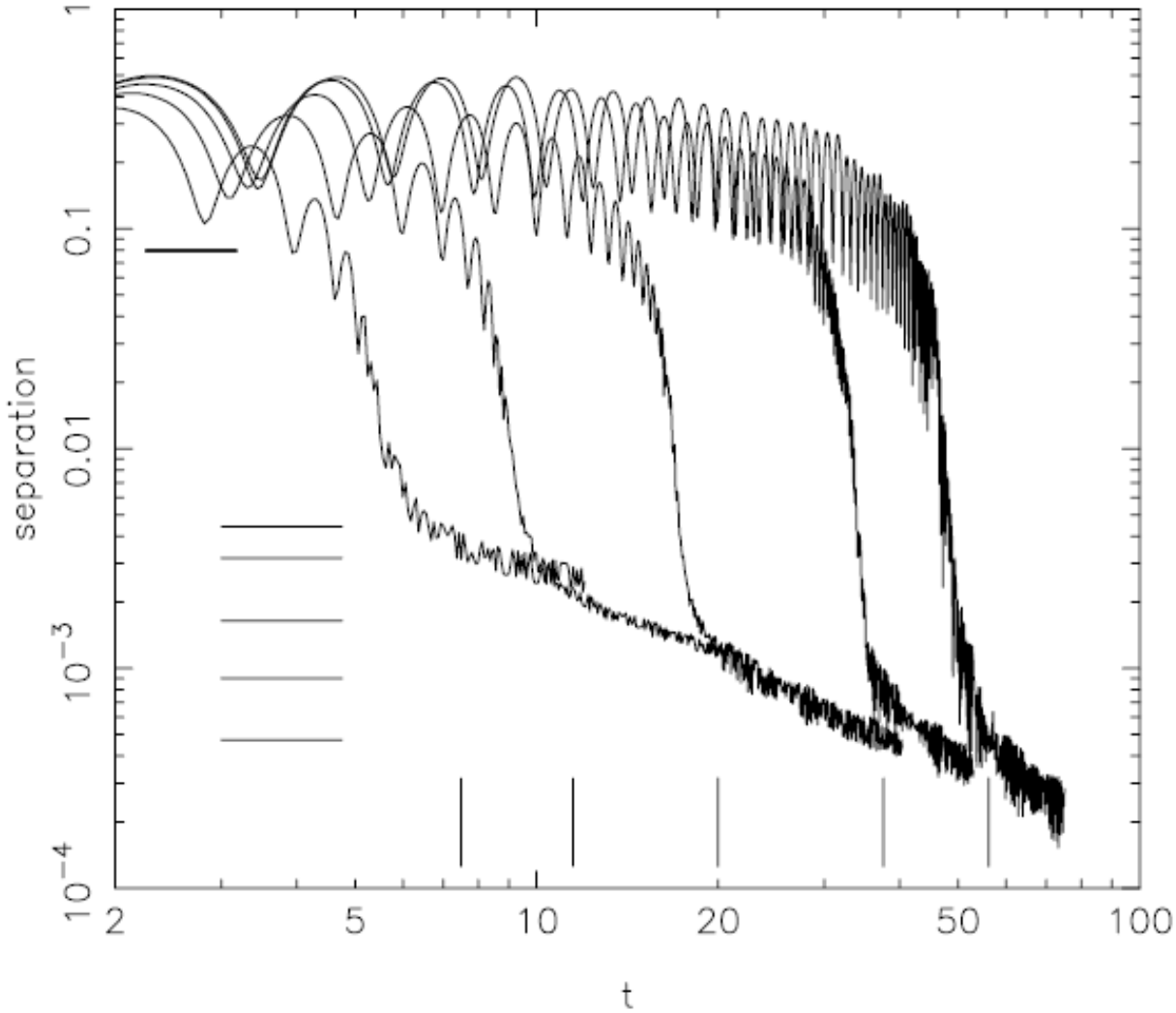

Figure: The binary separation as a function of time. Unit of separation is the radius of influence of the primary BH, unit of time is galaxy half-mass crossing time. Left to right is decreasing mass ratio. Figure taken from Merritt (2006).

Our Model

Stellar Dynamics

- Adding the precession rates due to the LK mechanism, stellar potential, and general relativity, we obtain an expression for the total precession rate:

$$\frac{d\omega}{d\tau} = \frac{3}{4I}\left[2I^2 + 5\sin^2\ \omega(e^2 - \sin^2 \imath)\right] - \kappa I + \frac{B}{I^2}\ ,$$

where

$$\kappa = \nu G_M(e,\gamma)\left[\frac{M_*(a)}{M_1}\right] T_K$$

is a measure of the strength of the stellar potential, and

$$B = \frac{3(GM_1)^{3/2}}{a^{5/2}c^2} T_K$$

is a measure of the strength of GR.

- The corresponding Hamiltonian is the integral of $\frac{d\omega}{d\tau}$ with respect to I:

$$H = \frac{1}{8}\left[-5 + 3I^2 + 3\sin^2 i(I^2 + 5e^2\sin^2\omega)\right] - \frac{\kappa I^2}{2} - \frac{B}{I}\ .$$

- As the Hamiltonian in once again cyclic in Ω, l_z is conserved:

$$\Lambda = l_z = \sqrt{1-e^2}\cos i \ .$$

- Using the constancy of the Hamiltonain , we obtain a second conserved quantity

$$e^2\left(5\sin^2\omega\sin^2 i - 2 + \frac{4\kappa}{3}\right) - \frac{8B}{3\sqrt{1-e^2}} = \text{const} = Q$$

- For notational convenience, we redefine $4\kappa/3 \to \kappa$ and $8B/3 \to B$. Letting e_+ and e_- be the maximum and minimum eccentricities, we have

$$\sin^2 i_+ = 1 - \frac{\Lambda^2}{1-e_+^2} \ ,$$

$$\sin^2 i_- = 1 - \frac{\Lambda^2}{1-e_-^2} \ .$$

- Solving for Λ^2,

$$\Lambda^2 = \frac{3+k}{5}(1-e_+^2)(1-e_-^2) - \frac{B}{5}\left(\frac{\left(\sqrt{1-e_-^2}-\sqrt{1-e_+^2}\right)\sqrt{(1-e_+^2)(1-e_-^2)}}{e_+^2-e_-^2}\right) .$$

- Since this is one equation with two variables, we don't have a single solution for e_+ and e_-, rather we have a region of space in the e_+, e_- plane where the above equation is valid. The above equation is solved numerically, and the largest value of e_+ and the smallest value of e_- are taken into account.
- From the value of e_+ and e_-, we obtain the smallest and largest angular momenta attained during the oscillation cycle:

$$l_- = \max(l_z, \sqrt{1-e_+^2}) \qquad l_+ = \sqrt{1-e_-^2} .$$

For the orbit to exist, we must have $l_+ > l_-$.

- In addition, librating orbits must have a fixed point in the $l - \omega$ space, i.e. a solution to

$$\frac{d\omega}{d\tau} = \frac{3}{4l}\left[2l^2 + 5(1 - l^2 - \sin^2 \imath)\right] - \kappa l + \frac{B}{l^2} = 0 \ .$$

  The solution of this is l_{fp}, the fixed point angular momentum. For librating orbits to exist, we must have $0 < l_{fp} < 1$.

- It is convenient to visualize the oscillations in angular momentum using contour plots of constant Q in $\omega - l$ axes. We can see that at large binary separations ($D \lesssim 1\mathrm{pc}$) the stellar potential precession destroys the Kozai oscillations, whereas for small separations ($D \gtrsim 0.05\mathrm{pc}$) GR does the same. There seems to be a "sweet spot" where the two effects cancel out, allowing the Kozai effect to dominate.

- The time period of these oscillations can be expressed in terms of the minimum and maximum angular mometa reached during the cycle:

$$P_k = \frac{8}{3\sqrt{6}} \frac{K(k^2)}{\sqrt{z_1 - z_3}} T_k \ ,$$

where,

$$\begin{aligned} z_1 &= 1 - I_-^2 \ , \\ z_2 &= 1 - I_+^2 \ , \\ z_3 &= -\frac{3}{2}(1 - I_+^2)\left(1 - \frac{I_{fp}^2}{I_+^2}\right) \ , \\ k^2 &= \frac{z_1 - z_2}{z_1 - z_3} \ , \end{aligned}$$

and $K(k^2)$ is the complete elliptic integral of the first kind with modulus k.

- The ratio P_K/T_K ranges from $\sim 1 - 10$.

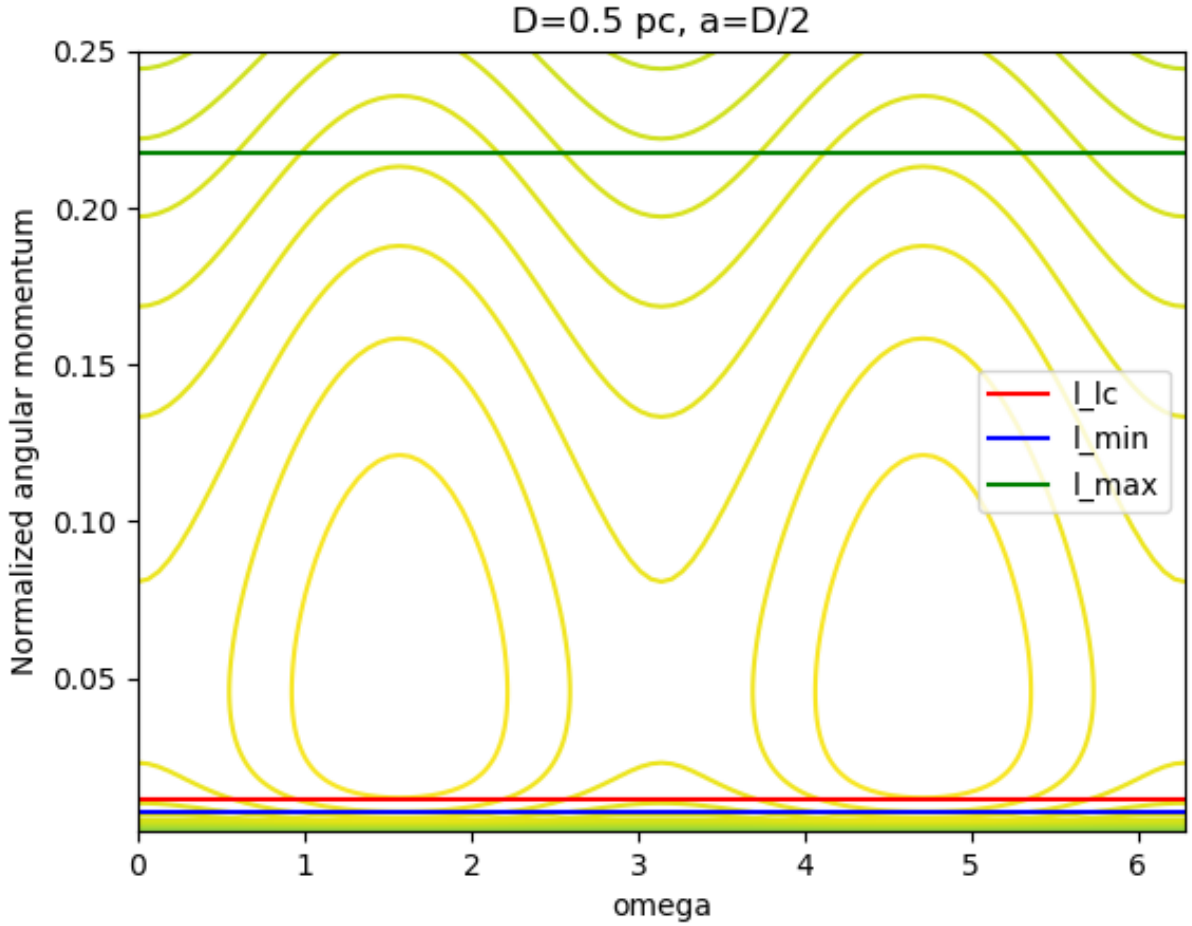

Figure: Contour plot of constant Q in the $\omega - I$ plane, for $D = 0.5$ pc, $a = D/2$. The parameters are $M_1 = 10^7 M_\odot$, $q = 0.01$, $\eta r_0 = 1$ pc, $\gamma = 1.5$. The angular momentum oscillates from ~ 0.01 to 0.22.

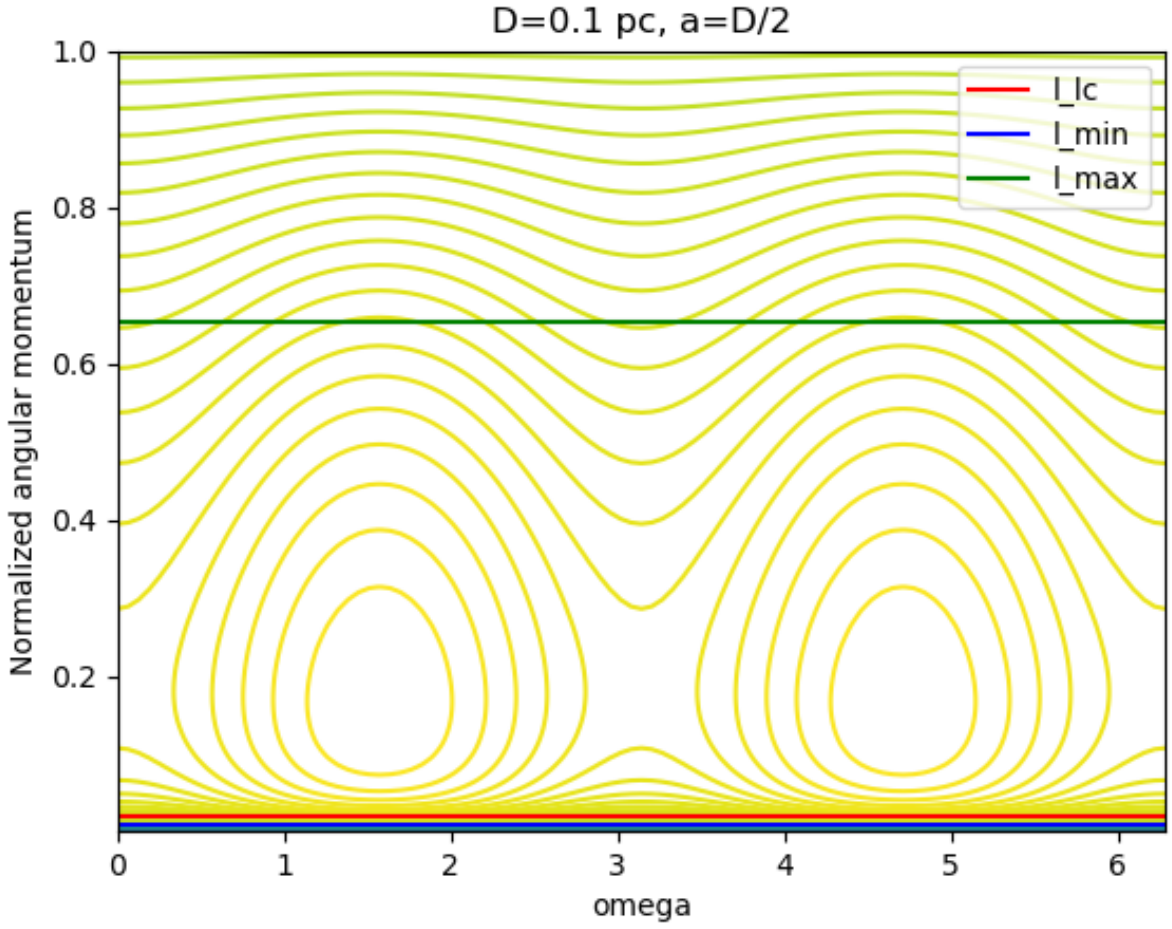

Figure: Similar plot, at a binary separation of 0.1 pc. Note that the Kozai effect is much stronger, allowing a greater oscillation of l. Other parameters are the same.

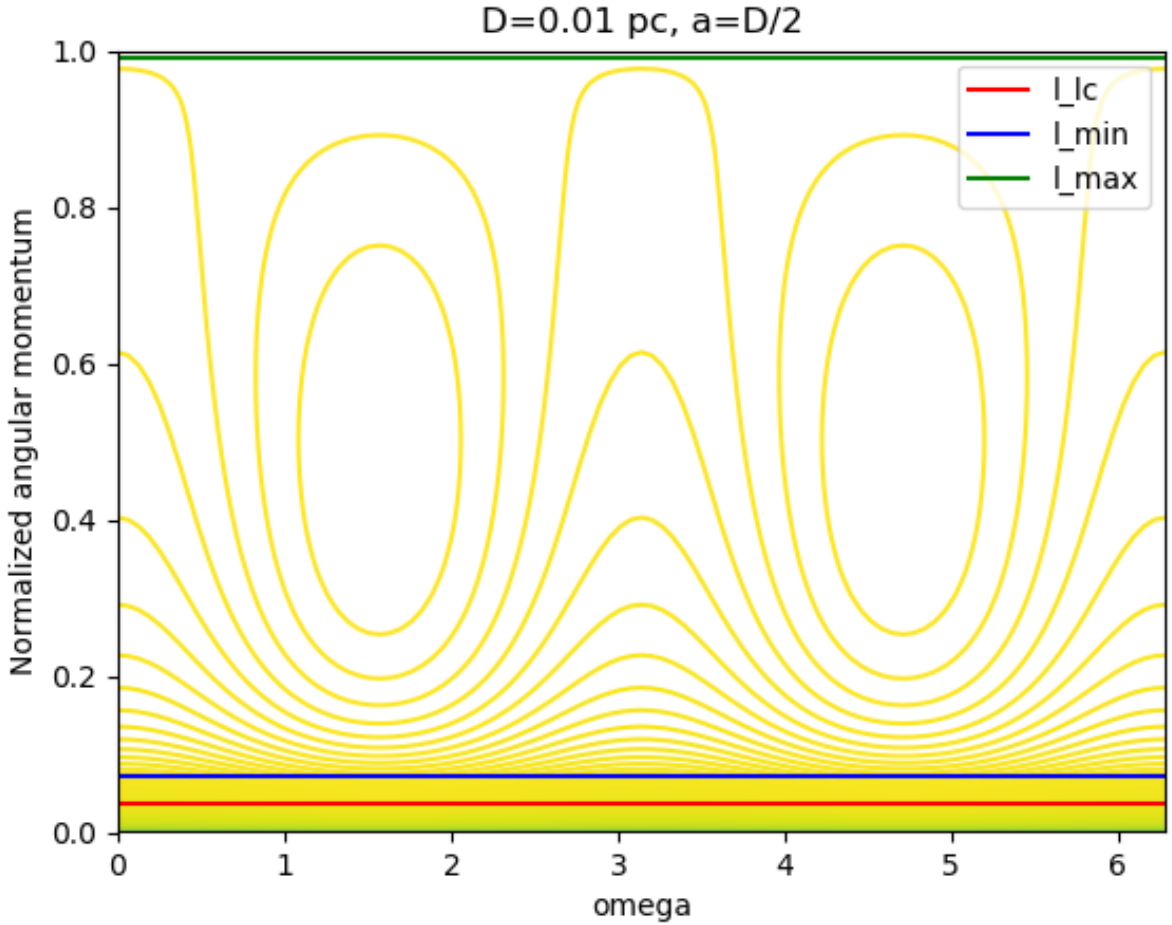

Figure: Similar plot, at a binary separation of 0.01 pc. Due to GR effects, the value of l_{min} is greater than l_{lc}, so the Kozai oscillations cannot drive stars into the loss cone . Other parameters are the same.

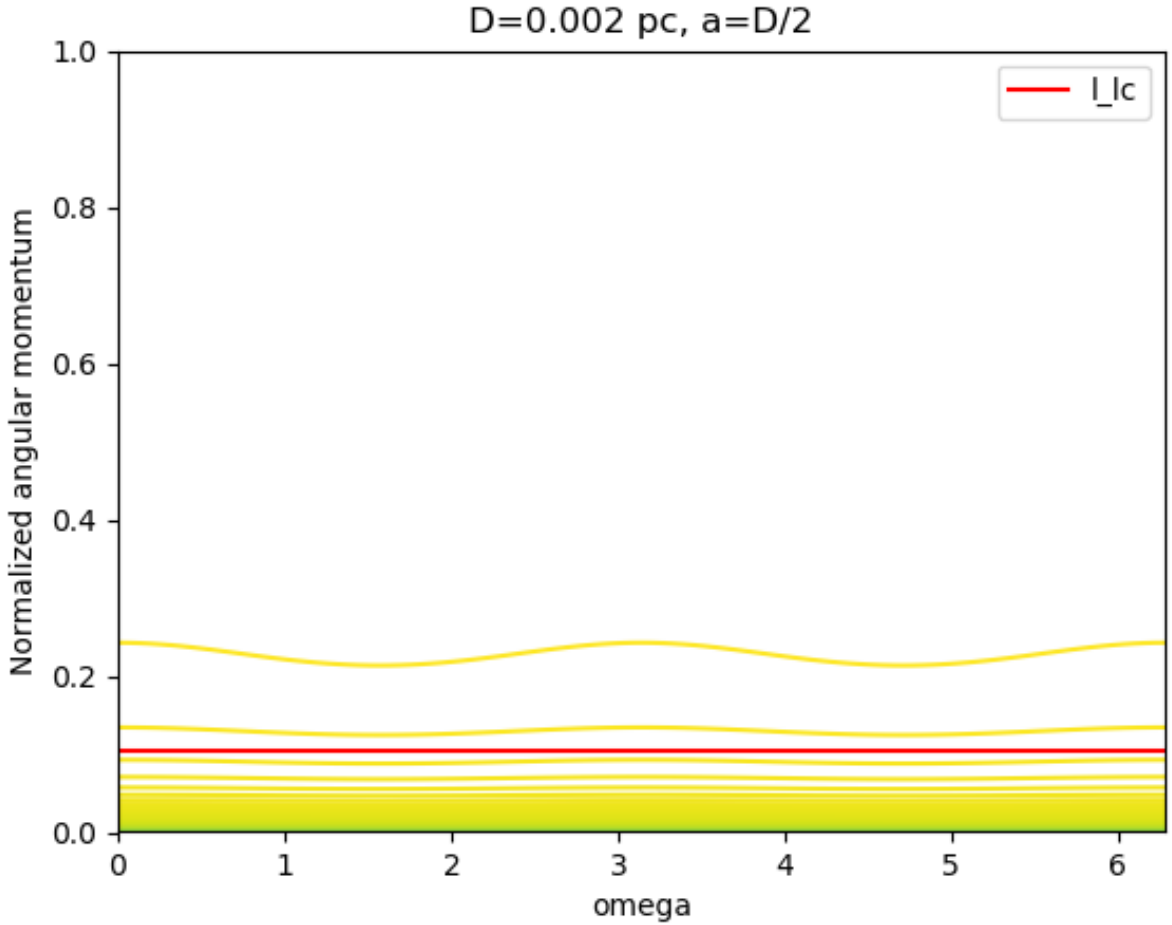

Figure: Similar plot, at a binary separation of 0.002 pc. The Kozai oscillations are almost completely suppressed due to the strong GR effects. Other parameters are the same.

- In the case of a single black hole in spherical geometry, a star enters the loss cone only if $l < l_{lc}$.
- However, in our system of a binary black hole, a star's angular momentum oscillates between l_+ and l_- while conserving l_z. Therefore, it can enter the loss cone as long as $l_- < l_{lc}$.
- This essentially transforms the loss cone into a loss wedge. Therefore, the presence of the secondary BH allows for a greater flux into the loss cone.
- The timescale of these oscillations are of the order of the Kozai timescale $T_K \sim 10^7 - 10^8$ yr, which is much smaller than the two-body relaxation timescale.

Capture Rate Calculation

- We assume that we are in the diffusive (empty) loss cone regime. The flux per unit energy is then given by

$$F(E)dE = \frac{N_{lw}(E)dE}{\tau_{relax}},$$

where $N_{lw}(E)$ is the number of stars in the loss wedge with energy E.

- We assume an isotropic power law distribution function, i.e. $f(E, \mathcal{R}, \mathcal{R}_z) = f(E) = CE^p$. The corresponding mass density is given by $\rho = \rho_0 \left(\frac{r}{r_0}\right)^{-\gamma}$, where $\gamma = p + 3/2$. Here, C is a normalization constant given by $C = 2^{-5/2}\pi^{-1}\left(\frac{GM_1}{r_0}\right)^{-p-3/2} \frac{n_0}{\beta(3/2, p+1)}$ where n_0 is the number density of stars at r_0.
- We define the radius of influence r_h of M_1 as the radius at which the mass enclosed is equal to the BH mass; $M_*(< r_h) = M_1$.
- The radius of influence is related to the cusp radius by $r_h = \eta r_0$, with η of order unity.

- It is convenient to convert this to a distribution over semimajor axes instead.

$$f(a) = f(E)\left|\frac{dE}{da}\right| = C\frac{GM_1}{2a^2}\left(\frac{GM_1}{2a}\right)^p \ .$$

- The number of stars inside the loss wedge is then given by

$$\begin{aligned} N_{lw}(a)da = \int\int \mathcal{G}_E f(a,l,l_z)da\,dl\,dl_z &= \mathcal{G}_E f(a)da\int_{l_-}^{l_+} dl\int_{-l_t}^{l_t} dl_z \\ &= 2\mathcal{G}_E f(a)\,(l_+ - l_-)\,l_t\,da \end{aligned}$$

provided that $l_- < l_t$. Here, the integration variables separate out because we are considering spherical symmetry. $\mathcal{G}_E$ is the density of states in spherical (isotropic) geometry:

$$\mathcal{G}_E = \frac{\sqrt{2}\pi^3(GM_1)^3}{E^{5/2}} = 8\pi^3(GM_1)^{1/2}a^{5/2} \ .$$

- For a SMBHB, the loss cone is never at a completely steady state, because the secondary BH is continuously inspiraling towards the center. In addition, the stellar cusp around the BH can significantly change during the inspiral, altering the stellar potential. The captures themselves lead to increase of the mass of the BH, which changes the size of the loss cone.
- However, if the change to the loss cone size and the stellar cusp is slow enough, they can be treated as adiabatic invariants, and the theory of steady state loss cone dynamics can be applied. The quasi-steady state assumption is assumed here, and is valid to a large degree

- Substituting for $N_{lw}(a)$ and $P(K)(a, D)$, we obtain an expression for the capture flux per unit semimajor axis:

$$F(a, D) = C' \; G^{1/2} q M_1^{5/3} m_*^{-7/6} (\eta r_0)^{p-3/2} r_*^{1/2} D^{-3} (I_+ - I_-) a^{3/2-p}$$

where C' is a numerical factor equal to $\frac{2^{-p-1}\pi(3/2-p)}{f_K \beta(3/2, p+1)}$.

- The total flux is obtained by integrating over semimajor axis. We take the upper limit of integration to be $D/2$, as the quadrupolar term in the Hamiltonian scales as $\frac{a^2}{D^3}$.

$$\dot{N}(D) = C' \; G^{1/2} q M_1^{5/3} m_*^{-7/6} (\eta \; r_0)^{p-3/2} r_*^{1/2} D^{-3} \int_0^{D/2} (I_+ - I_-) a^{3/2-p} da$$

- We scale the integrand with respect to D:

$$\dot{N}(D) = C' G^{1/2} q M_1^{5/3} m_*^{-7/6} (\eta r_0)^{p-3/2} r_*^{1/2} D^{-1/2-p} \int_0^{1/2} (I_+ - I_-) x^{3/2-p} dx$$

- The above expression is added to the flux due to two-body relaxation to get the total capture rate:

$$\dot{N}_{tot} = \dot{N}_B + \dot{N}_S \; ,$$

where B stands for binary and S stands for single.

Peak Capture Rate

- The deciding factor in the value of the capture rate is $(I_+ - I_-)$. In general, this is a complex function of D, a, κ, B among others.
- In order to estimate the peak capture rate, we assume that at an appropriate value of $D = D_p$, we have $I_+ \approx 1$ and $I_- \approx 0$. Therefore, we have

$$\dot{N}_p = \frac{(3/2-p)2^{-7/2}\pi}{(5/2-p)f_K\beta(3/2,p+1)} G^{1/2} q M_1^{5/3} m_*^{-7/6} (\eta r_0)^{p-3/2} r_*^{1/2} D_p^{-1/2-p}$$

$$= \frac{(3-\gamma)2^{-7/2}\pi}{(4-\gamma)f_K\beta(3/2,\gamma-1/2)} G^{1/2} q M_1^{5/3} m_*^{-7/6} (\eta r_0)^{\gamma-3} r_*^{1/2} D_p^{1-\gamma}$$

- When does this peak occur? We expect that when the two competing mechanisms, stellar potential precession and GR precession, cancel each other out, the Kozai mechanism will dominate and allow for a large oscillation in angular momentum.
- This means that the value of D_p is the solution to

$$\left(\frac{d\omega}{dt}\right)_{SP} + \left(\frac{d\omega}{dt}\right)_{GR} = 0$$

Assuming a typical value of $D_p = 2a_p$, we have

$$D_p = 2\left(\frac{3GM_1^{3/4}}{2^{3/4}c^2}(\eta r_0)^{3-\gamma}\frac{m_*^{1/4}}{r_*^{3/4}}\right)^{1/(\frac{13}{4}-\gamma)}$$

- We can use these expressions to obtain an approximate result for the capture rate vs time.

$$\frac{\dot{N}(t)}{\dot{N}_p} = 2^{5/2-p}\,(5/2-p)\left(\frac{D}{D_p}\right)^{-1/2-p}\int_0^{1/2}(I_+ - I_-)x^{3/2-p}dx\ .$$

- The value of the integral was analyzed as a function of D and the input parameters. The best fit curve is

$$\int_0^{1/2}(I_+ - I_-)x^{3/2-p}dx = \begin{cases} \frac{cd^{1.5}}{5.36+d^3} + k & D_{min} \le D \le D_{max} \\ 0 & \text{otherwise} \end{cases}$$

where $d = D/D_p$, and c and k are functions of the input parameters, of the order $c \sim 10^{-1}$ and $k \sim 10^{-2}$. D_{min} and D_{max} the starting and ending separations of the enhanced phase, described the next section.

- Therefore, the capture rate during the enhanced phase ($D_{min} \le D \le D_{max}$) is approximated by

$$\frac{\dot{N}(t)}{\dot{N}_p} = 2^{5/2-p}\,(5/2-p)\,d^{-1/2-p}\left(\frac{cd^{1.5}}{5.36+d^3} + k\right)\ .$$

Starting and Ending Points of the Enhanced Phase

- The changes in angular momentum due to the Kozai mechanism take place on a timescale $t_k = \left(\frac{1}{L}\frac{dL}{dt}\right)^{-1} = T_K\sqrt{1-e^2}$.
- Since the dynamics at large distances is dominated by stellar potential precession, we expect the enhanced phase to start when the Kozai timescale becomes smaller than the SP precession timescale.

$$\frac{\pi M_1}{\sqrt{1-e^2}}\frac{3-\gamma}{4\pi\rho_o a^3}\left(\frac{a}{r_0}\right)^{\gamma}\sqrt{\frac{a^3}{GM_1}}\frac{1}{G_M(e,\gamma)} > \sqrt{1-e^2}\frac{\sqrt{M_1}}{\sqrt{G}M_2}\frac{D^3}{a^{3/2}}$$

$$D_{max} = \left(\frac{\pi}{2^{\gamma}}\right)^{1/(3-\gamma)}\left(\frac{q}{0.01}\right)^{1/(3-\gamma)}\left(\frac{r_0\eta}{1\ \mathrm{pc}}\right) \quad \mathrm{pc}$$

- On the other hand, when the binary separation is in the sub-parsec scales, GR will be the dominating mechanism. The minimum value of D of the enhanced phase can be estimated by considering again the cancellation between SP and GR effects:

$$a_{min} = \left(\frac{3GM_1}{I^{3/2}c^2} (r_0\eta)^{3-\gamma} \right)^{1/(4-\gamma)}$$

Assuming a typical value of $I = 0.1$ and $D_{min} = 2a_{min}$,

$$D_{min} = 2 \left(\frac{3GM_1(r_0\eta)^{3-\gamma}}{c^2(0.1)^{3/2}} \right)^{1/(4-\gamma)}$$

- The duration of the enhanced phase is given by the time taken for the binary separation to shrink from D_{max} to D_{min}.

$$T_e = t_1 + t_2 + t_3$$

where

$$t_1 = \frac{max(D_{max}, r_h)^{3-\gamma/2} - r_h^{3-\gamma/2}}{\sqrt{\frac{G}{M_1}} M_2 \ln \Lambda (\eta r_0)^{\frac{3-\gamma}{2}} F(\gamma)(3-\gamma/2)}$$

$$t_2 = \frac{I \sigma_0 \eta^{\gamma-1}}{\mathcal{H} G \rho_0 r_0}$$

$$t_3 = \frac{1}{\mathcal{D}_0} \left(\frac{a_h^2}{min(a_h^2, D_{min}^2)} - 1 \right)$$

are the times spent in phase 1, 2, and 3 respectively.

- In most cases, $t_2 >> t_1, t_3$, implying the enhanced phase corresponds roughly to phase 2 (hardening phase) of the binary evolution.

Results

Parameter Space

- Throughout the work, we have assumed a power law density $\rho = \rho_0 \left(\frac{r}{r_0}\right)^{-\gamma}$, with r_0 being associated with the radius of influence of the BH r_h as $r_h = \eta r_0$. We recall that the radius of influence is defined as $M(< r_h) = M_1$. The value of ρ_0 is therefore determined by the parameters M_1, ηr_0, q, and γ.
- This density profile corresponds to an isotropic distribution function $f(E) = CE^p$ with $p = \gamma - 3/2$. We consider values of γ in the range from 0.7 to 1.9.
- There are several constraints on M_1 and q in our model. Firstly, a star's capture is observed as a tidal disruption event only if the tidal radius is greater than the Schwarzschild radius. This induces an upper limit of M_1 as $10^8 M_\odot$ for solar mass solar radius stars. Secondly, since M_2 is itself a supermassive black hole, qM_1 must be in the SMBH mass range.

- The Lidov-Kozai effect is applicable only to hierarchical three-body systems, so the value of q should be in the range range $0.01 - 0.1$. The values of M_1 are in the range $10^7 - 10^8 M_\odot$.
- The values of r_0 and η also have a wide range. We saw in the previous section that all the observables depend only on the combination $r_h = \eta r_0$. The radius of influence of Sagittarius A* is around 3 pc. We consider values of ηr_0 were taken to be from $0.5 - 5$ pc.

Table: Parameter space

Model No.	M_1	**q**	γ	ηr_0
1	$10^7 M_\odot$	0.01	1.75	1 pc
2	$10^7 M_\odot$	0.01	1.5	1 pc
3	$10^7 M_\odot$	0.01	1.2	1 pc
4	$10^7 M_\odot$	0.01	1	1 pc
5	$10^7 M_\odot$	0.01	0.7	1 pc
6	$10^7 M_\odot$	0.02	1.5	1 pc
7	$10^7 M_\odot$	0.03	1.5	1 pc
8	$10^7 M_\odot$	0.05	1.5	1 pc
9	$2 \times 10^7 M_\odot$	0.01	1.5	1 pc
10	$3 \times 10^7 M_\odot$	0.01	1.5	1 pc
11	$5 \times 10^7 M_\odot$	0.01	1.5	1 pc
12	$10^8 M_\odot$	0.01	1.5	1 pc
13	$10^7 M_\odot$	0.01	1.5	0.5 pc
14	$10^7 M_\odot$	0.01	1.5	2 pc
15	$10^7 M_\odot$	0.01	1.5	3 pc
16	$10^7 M_\odot$	0.01	1.5	5 pc

Capture Rate vs Time

The capture rate and the binary separation as a function of time for model 2 (q=0.01, $M_1 = 10^7 M_\odot$, $\gamma = 1.5$, $\eta r_0 = 1$ pc) are shown:

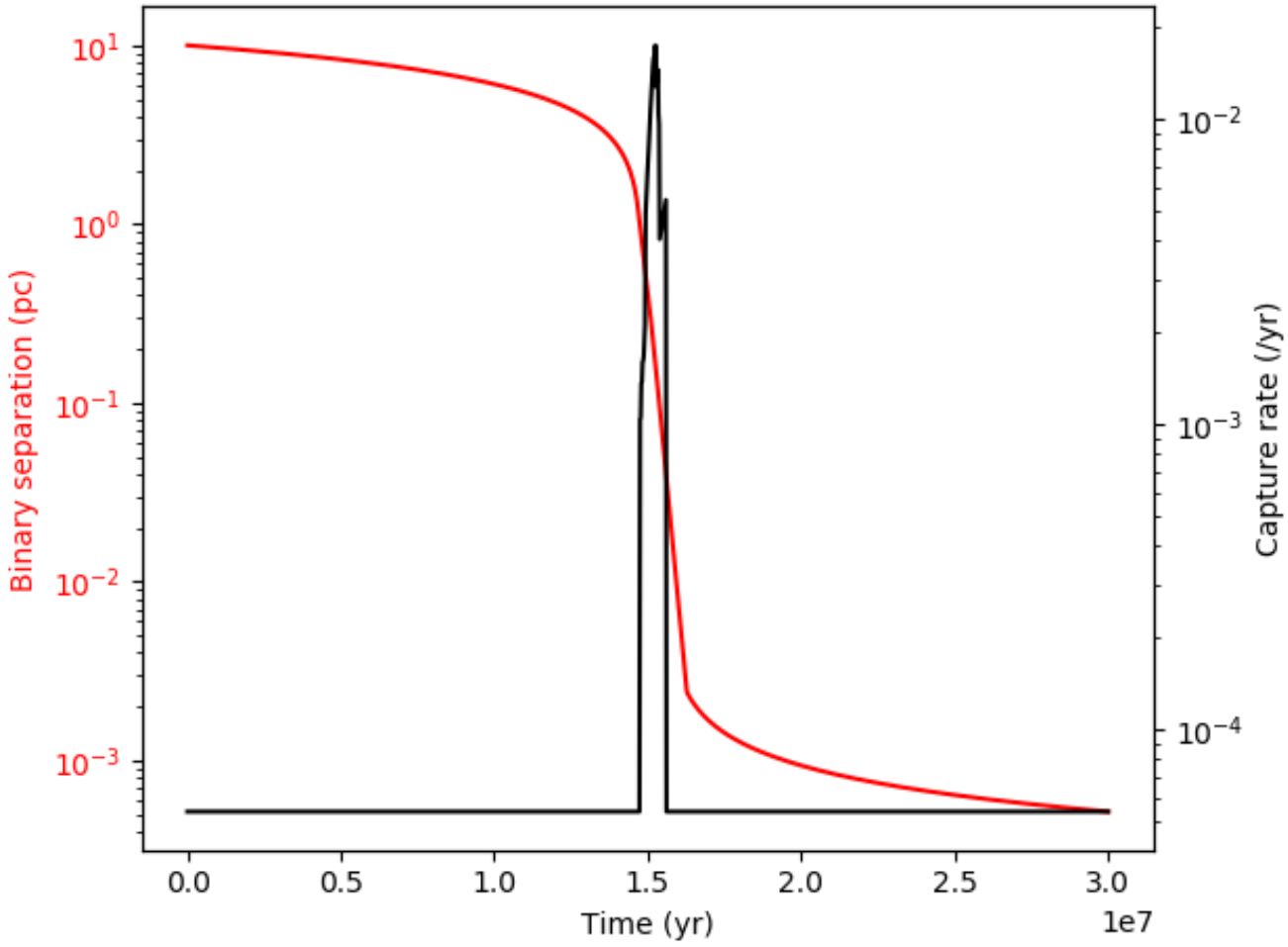

Figure: Left: binary separation in pc. Right: capture rate (/yr)

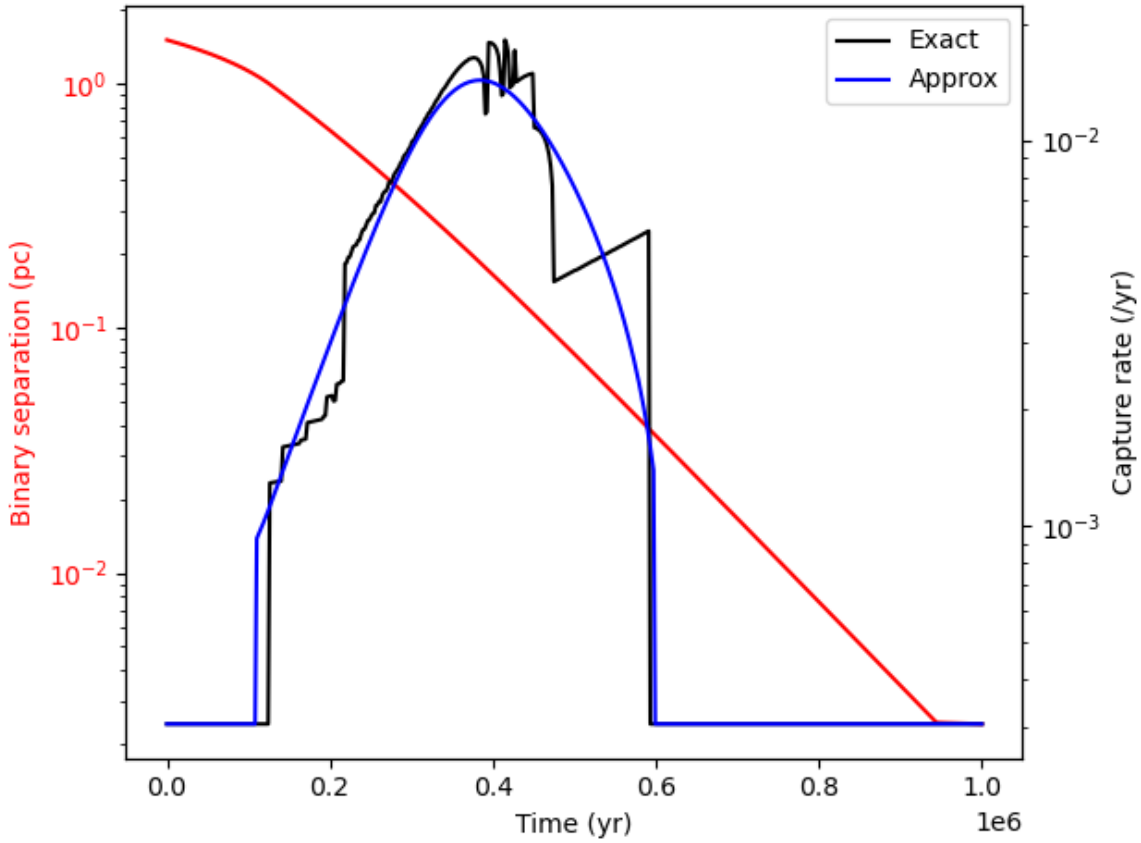

Figure: Zoomed in image of the previous figure, along with the approximation to the integral $\int_0^{1/2}(I_+ - I_-)x^{3/2-p}dx$.

The sudden and sharp rise and fall of the capture rate are due to our condition that a capture occurs only if $I_{min} \leq I_{lc}$. In reality, if $I_{min} \gtrsim I_{lc}$, the star can undergo complex chaotic three-body interaction with the binary system which may or may not result in a TDE.

Table: Results of the full model and analytic approximations for the various parameter choices listed earlier.

Model	Full Model					Approximation				
	$\dot{N}_p$ (/yr)	D_p (pc)	D_{max} (pc)	D_{min} (pc)	T_e (Myr)	$\dot{N}_p$ (/yr)	D_p (pc)	D_{max} (pc)	D_{min} (pc)	T_e (Myr)
1	0.045	0.1034	0.8686	0.0251	0.3876	0.0499	0.0822	0.9468	0.0238	0.4081
2	0.0176	0.1694	0.9955	0.0394	0.4602	0.0172	0.1297	1.0725	0.0371	0.4826
3	0.0069	0.2392	1.1141	0.0575	0.5598	0.0059	0.1936	1.1899	0.0569	0.5833
4	0.0037	0.2851	1.1844	0.0722	0.632	0.0029	0.2382	1.2533	0.0721	0.6571
5	0.0011	0.4358	1.2638	0.0853	0.8262	0.0008	0.306	1.3321	0.0975	0.788
6	0.0434	0.1658	1.5757	0.0209	0.3452	0.0344	0.1297	1.7025	0.0371	0.3304
7	0.0765	0.1668	2.0663	0.0109	0.322	0.0516	0.1297	2.2309	0.0371	0.2972
8	0.1662	0.2095	2.9048	0.005	0.2598	0.086	0.1297	3.1361	0.0371	0.2949
9	0.0459	0.1821	1.0035	0.0627	0.2318	0.0471	0.1746	1.0725	0.049	0.2596
10	0.0795	0.213	1.0087	0.0815	0.1544	0.0848	0.2077	1.0725	0.0576	0.1803
11	0.155	0.286	1.0201	0.1063	0.0941	0.1781	0.2585	1.0725	0.0706	0.1137
12	0.3849	0.2849	1.0492	0.1505	0.0489	0.4875	0.348	1.0725	0.0932	0.0606
13	0.0609	0.091	0.4985	0.0254	0.1071	0.0655	0.0716	0.5363	0.0245	0.1132
14	0.0054	0.2588	1.9833	0.0556	2.0153	0.0045	0.235	2.145	0.0562	2.0554
15	0.0027	0.327	2.9819	0.0662	4.8018	0.0021	0.3326	3.2175	0.0717	4.7939
16	0.0011	0.4377	4.02	0.0863	13.1989	0.0008	0.5153	5.3626	0.0974	13.9191

We see that the general trend of the calculations is as follows:

- The enhanced capture rate phase begins when the binary separation reaches $\sim r_h$.
- The enhanced phase ends when the binary separation reaches $\sim a_h$.
- The duration of the enhanced phase is generally of the order of $\sim 10^5 - 10^6$ yr. The duration is a strong function of ηr_0.
- As the mass ratio q increases, the value of D_{max} increases and D_{min} decreases. This is because the Kozai effect is more powerful, and can remain effective for a larger range of D. However, with increasing q, M_2 inspirals towards M_1 faster, so the duration of the enhanced phase is of the same order of magnitude.
- The peak capture rate $\dot{N}_p$ is 2-3 orders of magnitude higher than the typical capture rate of nuclei containing a single SMBH. It is a strong function of all the four parameters.

Scaling Relations

Below, we have a log-log plot of $\dot{N}_p$ as a function of M_1 for different values of γ. The other parameters, q and ηr_0, are set as 0.01 and 1 pc respectively. The linear relation in the log-log plot shows the validity of the approximation $\dot{N}_p \propto M_1^{\frac{5}{3}+\frac{3(1-\gamma)}{13-4\gamma}}$.

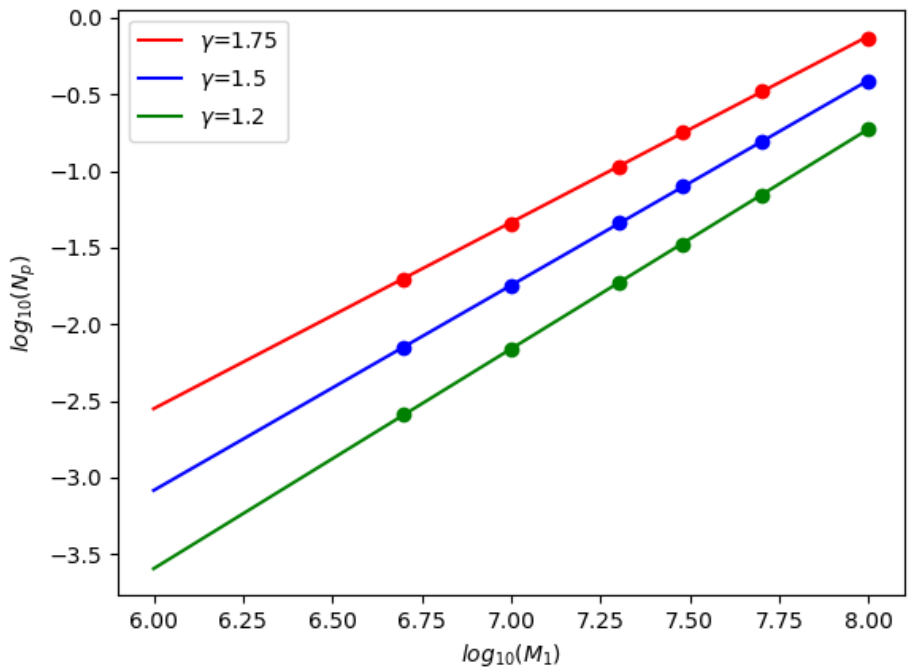

Figure: $log(\dot{N}_p)$ as a function of $log(M_1)$

Table: Slopes of $\log(\dot{N}_p)$ vs $\log(M_1)$

γ	**Best fit slope**	$\frac{5}{3} + \frac{3(1-\gamma)}{13-4\gamma}$
1.75	1.216	1.292
1.5	1.338	1.452
1.2	1.434	1.593

Next, we examine the relation between $\dot{N}_p$ and γ. The equation for N_p tells us that a plot of $log(\dot{N}_p)$ vs γ should be a straight line. The figure below confirms the validity of this result. The other parameters are set to $M_1 = 10^7 M_\odot$, $q = 0.01$, and $\eta r_0 = 1$ pc.

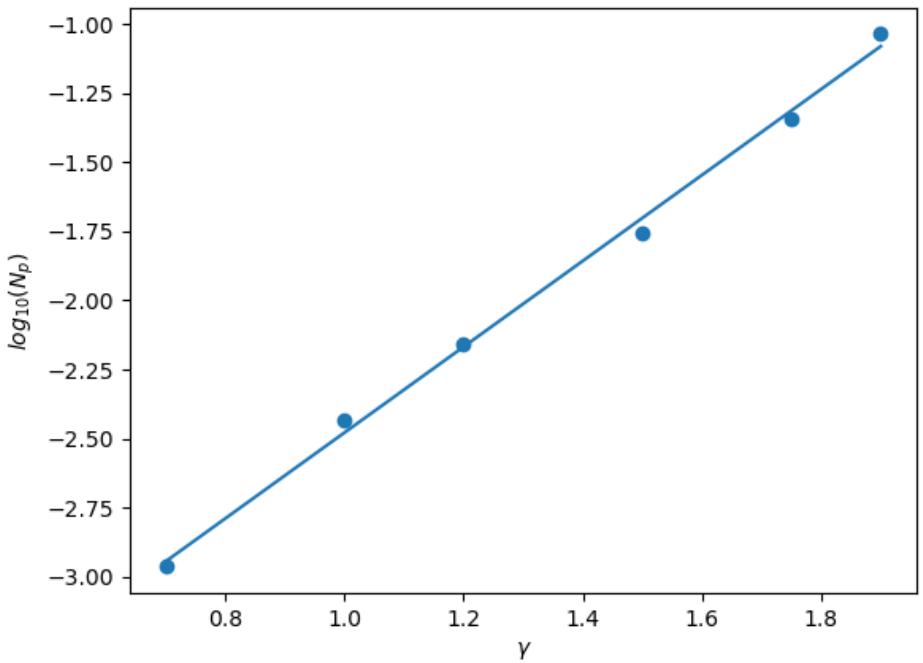

Figure: $\log(\dot{\mathrm{N}}_\mathrm{p})$ as a function of γ

In the figure below, $\dot{N}_p$ is plotted against q for different values of M_1. Our model and our data predict a linear relationship between the two, with $\gamma = 1.5$ and $\eta r_0 = 1$ pc. It is noted that our model is limited by the range of M_1 and q that we can explore.

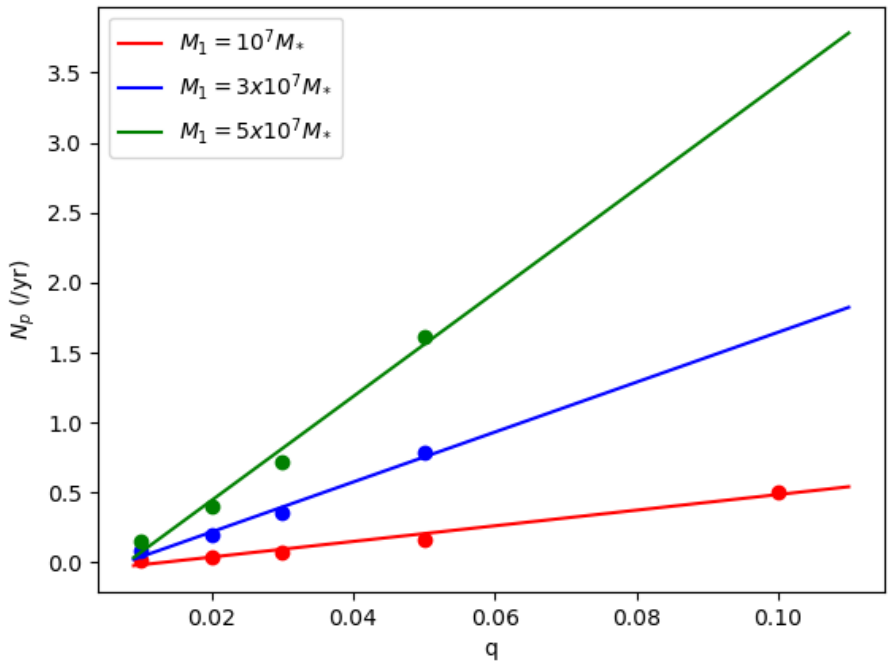

Figure: $\dot{N}_p$ as a function of q

Finally, we plot $\dot{N}_p$ as a function of $r_h = \eta r_0$. A plot of $log(\dot{N}_p)$ vs $log(r_h)$ should be a straight like with slope $(\gamma - 3) + \frac{4(3-\gamma)(1-\gamma)}{13-4\gamma}$. This is confirmed in the figure below. Solid line is for $M_1 = 10^7 M_\odot$, and dashed line is for $M_1 = 3 \times 10^7 M_\odot$.

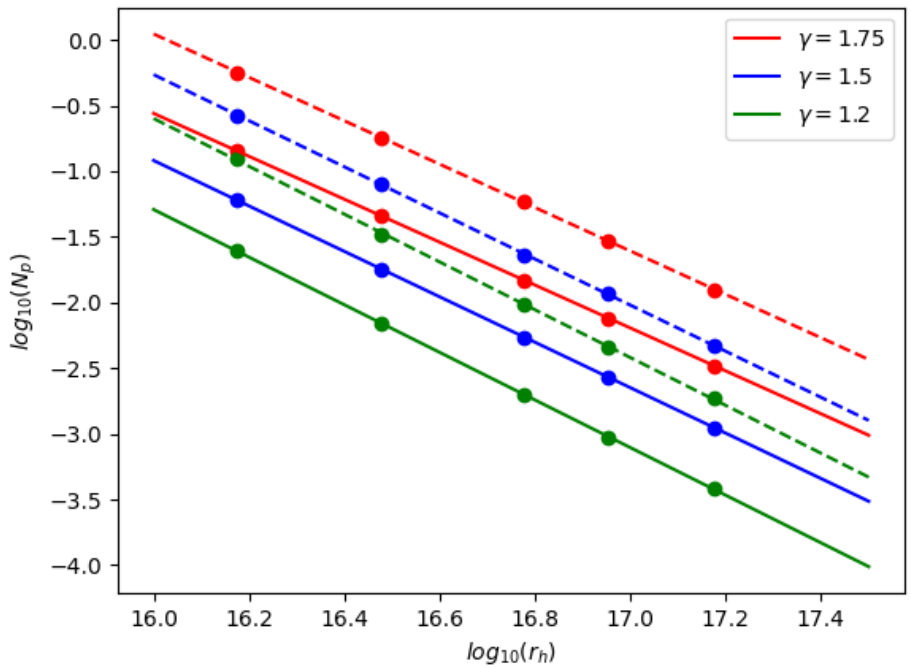

Figure: $\log(\dot{\mathrm{N}}_\mathrm{p})$ as a function of $\log(\mathrm{r}_\mathrm{h})$

Table: Slopes of $\log(\dot{N}_p)$ vs $\log(r_h)$

γ	**Slope for** $M_1 = 10^7 M_\odot$	**Slope for** $M_1 = 3 \times 10^7 M_\odot$	$(\gamma - 3) + \frac{4(3-\gamma)(1-\gamma)}{13-4\gamma}$
1.75	-1.634	-1.653	-1.875
1.5	-1.730	-1.755	-1.928
1.2	-1.813	-1.821	-1.976

Comparison with Other Studies

- Ivanov et. al. (2005) showed that for a dense cusp of size ~ 1 pc and $q \sim 0.01$, the TDE rate during the enhanced phase reaches about $10^{-2} M_\odot \ \mathrm{yr}^{-1}$. The duration of this enhancement was found to be $6 \times 10^4 \mathrm{yr}$. This is comparable to our model number 2, where the peak rate is 0.018 $M_\odot \ \mathrm{yr}^{-1}$ and the duration of enhancement is $4.6 \times 10^5 \mathrm{yr}$.
  For a value of $\gamma = 3/2$, they obtained a scaling relation of $\dot{N}_p \propto q^{4/3} M_1^{5/3} r_0^{-2}$. This can be compared to our expression of $\dot{N}_p \propto q M_1^{1.45} r_h^{-1.93}$ for $\gamma = 3/2$, which show similar scaling relations.
- Using numerical scattering experiments, Chen et. al. (2011) investigated the TDE rates of binaries entering the hardening stage, i.e. late half of phase 2. They obtained a scaling relation as $\dot{N}_p \propto q^{(4-2\gamma)/(3-\gamma)} \left(\frac{D}{a_h}\right) M_1^{-1/3} \sigma^4$. For a mass $M_1 = 10^7 M_\odot$ and $q = 1/81$ embedded in an isothermal cusp, they obtained a peak value of $\dot{N}_p \approx 0.2 \ \mathrm{yr}^{-1}$ for a duration of $\approx 3 \times 10^5 \ \mathrm{yr}$. This is comparable to our result of $\dot{N}_p \approx 0.1 \ \mathrm{yr}^{-1}$ for a duration of $3.4 \times 10^5 \ \mathrm{yr}$ when a value of $\gamma = 1.9$. A value of $\gamma = 1.5$ in their model gives the peak TDE rate as $\approx 10^{-2} \ \mathrm{yr}^{-1}$.

- Similar results were obtained from other studies by Lui and Chen (2013), Wegg and Bode (2013), Lezhnin and Vasiliev (2019), all of which showed a two-three order of magnitude increase in the capture rate for a short period of time.
- In summary, the results of our model match reasonably well with other models, and the scaling relations we have developed are comparable to their scaling relations. A complete extrapolation from our model to other direct numerical simulations require analysis of chaotic orbits that interact strongly with the binary system. However, the effectiveness of the Kozai mechanism, and its suppression by GR and stellar potential effects, is evident from our analytical model, and match well with existing results.

Conclusion

- In this project, we have examined the stellar capture rates in galactic nuclei containing a supermassive binary black hole with unequal masses. Such a setup is representative of the late stages of a minor merger.
- The field stars move under the influence of the primary and secondary BHs, gravitational effects of the cusp, and general relativity. The stellar dynamics of the field stars is very interesting, with our primary investigation being the angular momentum oscillations due to the Lidov-Kozai effect, stellar precession, and general relativity.
- There is a short window of time when the stellar potential precession and GR precession cancel each other, allowing the LK effect to dominate.

- We have developed analytic results for the peak capture rate and the duration of enhancement.
- Our general results show that the TDE rate is increases by two to three orders of magnitude compared to TDE rates of isolated black holes, and the duration of this enhanced phase is $10^5 - 10^6$ years.
- Enhanced TDE rates in galactic nuclei can be used as a method to identify minor mergers. Multiple TDEs originating in a nucleus that are observed during a survey indicate the possibility of the presence of a binary black hole

Scope for Further Studies

- Our model explores a limited range of parameters for the mass of the black holes, as the Lidov-Kozai mechanism is present in hierarchical three-body systems. In addition, tidal disruption events are observable only if the tidal radius is greater than the Schwarzschild radius, which sets an upper limit of M_1 as $\approx 10^8 M_\odot$. Further work include exploring a full range of parameters. Specifically, the TDE rates during major mergers, where the black holes are of comparable mass, is to be explored from an analytic point of view.
- From an observational point of view, an integral over the cosmic volume is to be performed, in order to calculate the number of TDEs which will be observable from Earth, and the fraction of the TDEs which originate in SMBHBs. The probability of a multiple-TDE galaxy hosting a SMBHB is to be calculated.
- Our novel analytical model may provide more accurate predictions for the observable TDE rates and lead to new exploration in the field of galaxy mergers.